



Magnetostatics of synthetic ferrimagnet elements

Olivier Fruchart, Bernard Dieny

► To cite this version:

Olivier Fruchart, Bernard Dieny. Magnetostatics of synthetic ferrimagnet elements. 2010. hal-00495463v1

HAL Id: hal-00495463

<https://hal.science/hal-00495463v1>

Preprint submitted on 26 Jun 2010 (v1), last revised 11 Jun 2011 (v2)

HAL is a multi-disciplinary open access archive for the deposit and dissemination of scientific research documents, whether they are published or not. The documents may come from teaching and research institutions in France or abroad, or from public or private research centers.

L'archive ouverte pluridisciplinaire **HAL**, est destinée au dépôt et à la diffusion de documents scientifiques de niveau recherche, publiés ou non, émanant des établissements d'enseignement et de recherche français ou étrangers, des laboratoires publics ou privés.

Magnetostatics of synthetic ferrimagnet elements

Olivier Fruchart

Institut NÉEL, CNRS & Université Joseph Fourier – BP166 – F-38042 Grenoble Cedex 9 – France^{a)}

Bernard Diény

SPINTEC (UMR8191 CEA/CNRS/UJF/G-INP), CEA Grenoble, INAC, 38054 Grenoble Cedex 9, France

(Dated: 26 juin 2010)

We calculate the magnetostatic energy of synthetic ferrimagnet (SyF) elements, consisting of two thin ferromagnetic layers coupled antiferromagnetically through RKKY coupling. We calculate exact formulas as well as approximate yet accurate ones, which can be used to easily derive energy barriers and anisotropy fields of SyF. These can be used to evaluate coercivity, thermal stability and other useful quantities.

Synthetic antiferromagnets^{1,2} consist of two thin ferromagnetic films of moments of same magnitude however strongly coupled antiferromagnetically thanks to the RKKY interaction present in an ultrathin metal spacer layer, typically Ru 0.6 – 0.9 nm-thick³. Hereon we will consider the more general case of practical use where the two antiparallel-coupled moments are of different magnitude, and name this a synthetic ferrimagnet (SyF). The purpose of SyFs is to provide (spin-polarized) ferromagnetic layers required in magneto-resistive or spin-torque devices, while displaying an overall weak moment. As originally proposed^{1,2} the first benefit of weak moments is to minimize cross-talk of neighboring (*e.g.* memory bits) or stacked (*e.g.* in a spin-valve⁴) elements through stray-field coupling. The second benefit is to minimize the effect of external field through Zeeman coupling, *e.g.* to strengthen the pinning in reference layers⁵ or minimize effects of the Oersted field in magneto-resistive or spin-torque oscillator devices.

In practice SyFs are used in the form of elements of finite lateral size. For single-layer elements shape anisotropy is often used to define an easy axis for the magnetization direction. For lateral size below typically 100 nm the coercivity and stability of information are dictated by the energy barrier in the transverse direction, which is reasonably described by in-plane demagnetizing coefficients through : $\Delta\mathcal{E}_d = (1/2)\mu_0 M_s^2 \Delta N V$. V is the volume of the element, M_s its spontaneous magnetization and ΔN is the difference between the two in-plane demagnetizing coefficients. While analytical expressions are available for such coefficients in single-layer flat elements^{6–11}, the evaluation of energy barriers and dipolar coupling in SyFs has not been discussed beyond the point-dipole approximation, which however is known to be very crude in flat elements as dipolar field are very short-ranged in two dimensions¹². In this Letter we report exact analytical expressions for the magnetostatics of SyFs uniformly-magnetized in each sub-layer. We discuss the physical meaning of the results, and propose approximate yet accurate expressions for their straight-

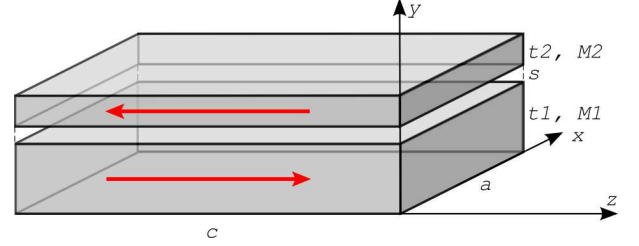


FIGURE 1. Geometry and notations of a prismatic SyF element comprising two ferromagnetic layers F_1 and F_2 .

forward evaluation.

Let us first consider SyF prisms and denote F_1 and F_2 the two ferromagnetic layers (FIGURE 1). Without loss of generality, we consider that the magnetization direction is along z . In the framework of magnetostatic charge and potential we apply the formulas of Rhodes and Rowlands expressing the interaction between two parallel charged surfaces⁷, and adopt the convenient notation of F_{ijk} functions, the i , j and k -fold indefinite integrals along x , y and z of the Green function $F_{000} = 1/r$ ¹³. The only such function needed here is

$$F_{220} = \frac{1}{2}[x(v-w)L_x + y(u-w)L_y] - xyP_z + \frac{1}{6}r(3w-r^2) \quad (1)$$

with $u = x^2$, $v = y^2$, $w = z^2$, $r = \sqrt{u+v+w}$, $L_x = (1/2) \ln[(r+x)/(r-x)]$ etc, $P_x = x \arctan(yz/xr)$ etc, and $L_x = 0$ and $P_x = 0$ for $x = 0$ etc.

The integrated magnetostatic energy of a single prismatic element of thickness t is :

$$\mathcal{E}_d = \frac{\mu_0 M_s^2}{\pi} \sum_{\delta_a, \delta_t, \delta_c \in \{0,1\}} (-1)^{\delta_a + \delta_t + \delta_c} F_{220}(a\delta_a, t\delta_t, c\delta_c) \quad (2)$$

which normalized to $(1/2)\mu_0 M_s^2$ yields the demagnetizing coefficient N_z . It can be checked that Eq. (2) coincides with the explicit formula already provided⁹. Based on this the integrated magnetostatic energy of the SyF element may be written :

^{a)} Electronic mail: Olivier.Fruchart@grenoble.cnrs.fr

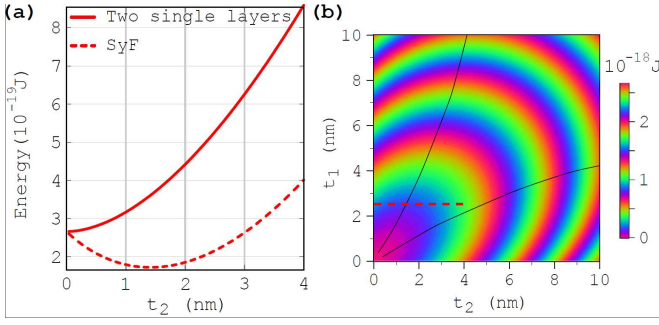


FIGURE 2. Magnetostatic energy of an SyF with $c = 2a = 100$ nm, $M_{1,2} = 10^6$ A/m, $s = 0.7$ nm. (a) Sum of the energies of two prisms without mutual interaction, and when embedded in the SyF geometry. t_1 is kept constant at 2.5 nm, while t_2 is varied. (b) Energy of the general SyF. Black lines are minimum energy line for either constant t_1 or t_2 . The red dotted line highlights the path for the SyF curve shown in (a).

$$\begin{aligned} \mathcal{E}_d = & \frac{1}{2}\mu_0 M_1^2 N_z(a, t_1, c)at_1c + \frac{1}{2}\mu_0 M_2^2 N_z(a, t_2, c)at_2c \\ & + \frac{\mu_0 M_1 M_2}{\pi} \sum_{\delta_1, \delta_2, \delta_a, \delta_c \in \{0,1\}} (-1)^{\delta_1 + \delta_2 + \delta_a + \delta_c} \\ & \times F_{220}(a\delta_a, s + t_1\delta_1 + t_2\delta_2, c\delta_c). \end{aligned} \quad (3)$$

FIGURE 2(a) shows the magnetostatic energy \mathcal{E}_d upon building a SyF via the progressive thickness increase of F2 above F1, considering or not the interaction between the two layers. In the latter case the energy increase nearly scales with t_2^2 , which is understandable because it is a self-energy (in F2 alone). In the SyF case \mathcal{E}_d first decreases linearly and then increases again. This can be understood as for low t_2 the extra edge charges induced by an infinitesimal increase δt_2 mainly feel the stabilizing stray field arising from F1, while for large t_2 they feel more the nearby charges induced by F2 itself. Notice that, contrary to what could be a first guess, for the SyF the minimum of $\mathcal{E}_d(t_2)$ occurs before the cancellation of moment at $t_1 = t_2$. This stems from the same argument as above, which is that magnetic charges at an edge of F2 are closer one another than to the charges on the nearby surface of F1, thus for an identical amount contribute more to \mathcal{E}_d .

FIGURE 2(b) shows the full plot of $\mathcal{E}_d(t_1, t_2)$ for $s = 0.7$ nm. The above arguments appear general. From this figure let us outline three take-away messages. 1. As a rough guideline, for fixed t_1 the magnetostatic energy of a SyF is found for $t_2 \approx t_1/2$. 2. At this minimum \mathcal{E}_d is reduced by only $\approx 20\%$ with respect to a single-layer element of thickness t_1 . 3. \mathcal{E}_d roughly regains its value of the single layer at the compensation point, for a true (Synthetic AntiFerromagnet, SAF, for $t_2 = t_1$).

These results shed light on results previously noticed empirically, however not explained. For instance Wiese

et al. noticed that the effective anisotropy of a SyF *basically scales with the inverse net moment*¹⁴. This arises from the similar energy of the SyF along the hard axis with respect to a single layer, while the Zeeman energy scales with the inverse net moment. Beyond their use to evaluate coercivity and energy barriers, the present expressions may be used *e.g.* to derive phase diagrams for vortex versus single-domain in disks^{15,16}, or vortex versus transverse domain walls in stripes made of trilayers^{17,18}. As an example Tezuka *et al.* investigated single-domain versus flux-closure states in micron-sized prismatic SyFs¹⁹. They noticed that *there is an optimum ferromagnetic film thickness at which SyAF can obtain a single-domain structure*: for $t_1 = 10$ nm and $s = 0.6$ nm a single-domain state was evidenced for $t_2 = 4, 6$ nm, while a flux-closure state was evidenced for $t_2 = 2, 8$ nm. This is in perfect agreement with the energy minima highlighted in FIGURE 2b. More quantitative arguments about such phase diagrams for SyFs will be provided in a forthcoming paper.

With a view to ease the use of the present accurate magnetostatics for SyF while eliminating the need for any numerical evaluation, in the following we derive approximate yet highly accurate expressions for \mathcal{E}_d . FIGURE 3a shows that to a very good approximation, \mathcal{E}_d is proportional to the width of the element (along x) and is independent of its length (along z), already for a single-layer *i.e.* with no moment compensation. This argument reaches a very high accuracy close the compensation $t_1 = t_2$ because edges appear as lines of dipoles, whose stray field quickly decays with distance ($\sim 1/r^2$). This allows us to boil down \mathcal{E}_d to a single line integral along its edge :

$$\mathcal{E}_d = E_\lambda \oint (\mathbf{m} \cdot \mathbf{n})^2 ds \quad (4)$$

$$= E_\lambda \oint \frac{|dx|}{\sqrt{1 + (\partial_x f)^2}} \quad (5)$$

$$= E_\lambda \int_0^{2\pi} \frac{(r \sin \theta - \partial_\theta r \cos \theta)^2}{\sqrt{(\partial_\theta r)^2 + r^2}} d\theta \quad (6)$$

Eq. (4) is the general expression, expressed in the following two lines in cartesian and polar coordinates (FIGURE 4a). E_λ is the density of magnetostatic energy per unit length of edge, a concept once discussed in the case of single layers²⁰, yet much more accurate here in the case of lines of dipoles, instead of monopoles. Equations (4-6) apply to an arbitrary shape (not simply prisms) by considering the in-plane angle φ between magnetization and the normal to the edge. It can be checked that for an SAF with F1 and F2 of identical magnetization and thickness, we have with an accuracy better than 10 % for geometrical parameters relevant for practical cases, *i.e.* $t_{1,2}$ in the range 2 – 10 nm and $s \in 0.5 - 1$ nm :

$$E_\lambda = (1/4)\mu_0 M_s^2 t^2 \quad (7)$$

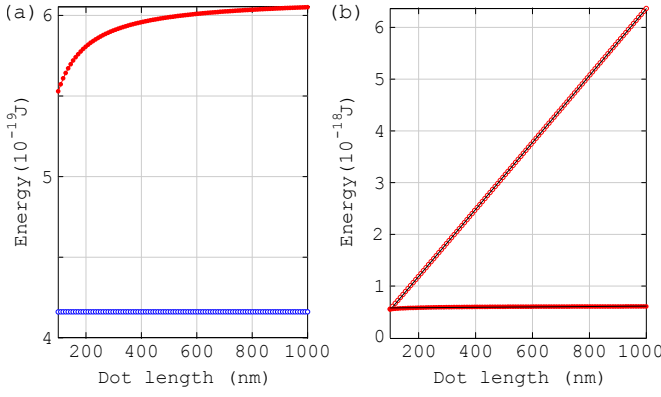


FIGURE 3. (a) Energy of a single layer (full symbols) and SyF (open symbols) as a function of dot length, *i.e.* along z , while $a = 100$ nm. (b) Energy of a single layer as a function of width (along x , open symbols), and length (along z , full symbols, same curve as in a), while the other in-plane dimension is kept constant at 100 nm. The lines are linear fits. For both plots the parameters are : $M_i = 10^6$ A/m, $t_1 = t_2 = 2.5$ nm, $s = 0.7$ nm.

The meaning of Eq. (7) is straightforward : due to the very short range of interaction between dipolar lines, the density of dipolar energy is non-zero only in the vicinity of the edges, with a lateral range t . Thus a volume t^2 is concerned with a line density of energy of the order $(1/2)\mu_0 M_s^2$, explaining the scaling of Eq. (7). Expressions for non-compensated cases (including single elements) may be evaluated numerically. This provides us with analytical expressions for the magnetostatics of SyFs for the most usual shapes (FIGURE 4b).

Using the point-dipole approximation as often found in literature, the energy gained by coupling F1 and F2 scales with $\mu_0 a E_\lambda (a/t)^3$, which obviously is largely incorrect with an extra scaling $(a/t)^3$ (see FIGURE 4a). The present formulas thus provide a major improvement over existing approaches.

To conclude we derived exact formulas for the magnetostatics of prism SyF, and simple yet accurate forms for SyFs of arbitrary shapes. These extend to SyF the concept of demagnetizing coefficients to SyF. These simple forms may be used straightforwardly to derive scaling laws for all aspects of SyF physics pertaining to dipolar energy such as thermal stability, coercivity, anisotropy field, or phase diagrams for critical size (*e.g.* single-domain versus vortex, transverse versus vortex wall).

RÉFÉRENCES

- ¹D. Heim and S. S. P. Parkin, "Us patent 5,465,185," (1995), magnetoresistive spin valve sensor with improved pinned ferromagnetic layer and magnetic recording system using the sensor.
- ²H. Van den Berg, "Us patent 5,686,838," (1997), magnetoresistive sensor having at least a layer system and a plurality of measuring contacts disposed thereon, and a method of producing the sensor.

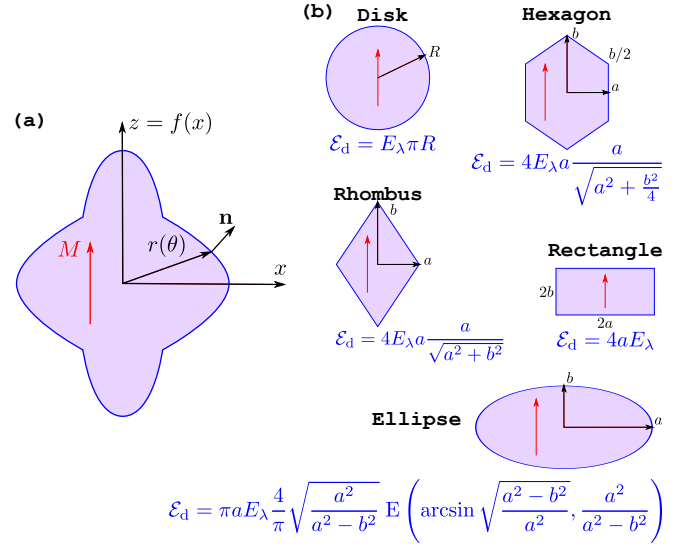


FIGURE 4. (a) notations for the calculation of edge energy (b) integrated magnetostatic energy for various shapes. E is the elliptical integral of the second kind. See text for the definition of E_λ .

- ³S. S. P. Parkin, "Systematic variation of the strength and oscillation period of indirect magnetic exchange coupling through the 3d, 4d, and 5d transition metals," *Phys. Rev. Lett.* , **67**, 3598–3601 (1991).
- ⁴B. Diény, V. S. Speriosu, S. S. P. Parkin, B. A. Gurney, D. R. Wilhoit, and D. Mauri, "Giant magnetoresistance in soft ferromagnetic multilayers," *Phys. Rev. B* , **43**, 1297 (1991).
- ⁵H. A. M. van den Berg, W. Clemens, G. Gieres, G. Rupp, W. Schelter, and M. Vieth, "Gmr sensor scheme with artificial antiferromagnetic subsystem," *IEEE Trans. Magn.* , **32**, 4624 (1996).
- ⁶J. A. Osborn, "Demagnetizing factors of the general ellipsoid," *Phys. Rev.* , **67**, 351–357 (1945).
- ⁷P. Rhodes and G. Rowlands, "Demagnetizing energies of uniformly magnetized rectangular blocks," *Proc. Leeds Phil. Liter. Soc.* , **6**, 191 (1954).
- ⁸D. X. Chen, J. A. Brug, and R. B. Goldfarb, "Demagnetizing factors for cylinders," *IEEE Trans. Magn.* , **27**, 3601 (1991).
- ⁹A. Aharoni, "Demagnetizing factors for rectangular ferromagnetic prisms," *J. Appl. Phys.* , **83**, 3432–3434 (1998).
- ¹⁰D. A. Goode and G. Rowlands, "The demagnetizing energies of a uniformly magnetized cylinder with an elliptic cross-section," *J. Magn. Magn. Mater.* , **267**, 373–385 (2003).
- ¹¹B. Borca, O. Fruchart, E. Kritisikis, F. Cheynis, A. Rousseau, Ph. David, C. Meyer, and J. Toussaint, "Tunable magnetic properties of arrays of fe(110) nanowires grown on kinetically grooved w(110) self-organized templates," *J. Magn. Magn. Mater.* , **322**, 257 (2010).
- ¹²O. Fruchart, J.-P. Nozières, W. Wernsdorfer, D. Givord, F. Rousseaux, and D. Decanini, "Enhanced coercivity in sub-micrometer-sized ultrathin epitaxial dots with in-plane magnetization," *Phys. Rev. Lett.* , **82**, 1305–1308 (1999).
- ¹³A. Hubert and R. Schäfer, *Magnetic domains. The analysis of magnetic microstructures* (Springer, Berlin, 1999).
- ¹⁴N. Wiese, T. Dimopoulos, M. Rührig, J. Wecker, and G. Reiss, "Switching of submicron-sized, antiferromagnetically coupled cofeb/ru/cofeb trilayers," *J. Appl. Phys.* , **98**, 103904 (2005).
- ¹⁵R. P. Cowburn, "Property variation with shape in magnetic nanoelements," *J. Phys. D: Appl. Phys.* , **33**, R1–R16 (2000).
- ¹⁶P. O. Jubert and R. Allenspach, "Analytical approach to the

- single-domain-to-vortex transition in small magnetic disks,” *Phys. Rev. B* , **70**, 144402/1–5 (2004).
- ¹⁷R. McMichael and M. Donahue, “Head to head domain wall structures in thin magnetic strips,” *IEEE Trans. Magn.* , **33**, 4167 (1997).
- ¹⁸Y. Nakatani, A. Thiaville, and J. Miltat, “Head-to-head domain walls in soft nano-strips : a refined phase diagram,” *J. Magn. Mater.* , **290-291**, 750 (2005).
- ¹⁹N. Tezuka, N. Koike, K. Inomita, and S. Sugimoto, “Magnetization reversal and domain structure of antiferromagnetically coupled submicron elements,” *J. Appl. Phys.* , **93**, 7441 (2003).
- ²⁰S. W. Yuan, H. N. Bertram, J. F. Smyth, and S. Shultz, “Size effects of switching fields of thin permalloy particles,” *IEEE Trans. Magn.* , **28**, 3171 (1992).